

${}^6\text{Li}$ structure information from ${}^2\text{H}(\alpha, \alpha){}^2\text{H}$ scattering

K. Massen-Hane, P. R. Fraser*, A. S. Kadyrov, I. Bray

*Department of Physics, Astronomy and Medical Radiation Sciences, Curtin University, GPO
Box U1987, Perth 6845, Australia*

*E-mail: kym.massen-hane@student.curtin.edu.au;
paul.fraser@curtin.edu.au; a.kadyrov@curtin.edu.au;
i.bray@curtin.edu.au*

K. Amos

School of Physics, University of Melbourne, Victoria 3010, Australia

Department of Physics, University of Johannesburg, P.O. Box 524, Auckland Park, South Africa

E-mail: amos@unimelb.edu.au

L. Canton

Istituto Nazionale di Fisica Nucleare, sezione di Padova, Padova I-35131, Italy

E-mail: luciano.canton@pd.infn.it

D. W. Drumm

*Australian Research Council Centre of Excellence for Nanoscale BioPhotonics, School of
Science, RMIT University, Melbourne, VIC 3001, Australia*

*Theoretical Chemical and Quantum Physics, School of Science, RMIT University, Melbourne,
VIC 3001, Australia*

E-mail: daniel.drumm@rmit.edu.au

In this study, we investigate low-energy elastic scattering of ${}^4\text{He}+{}^2\text{H}$ using an effective two-body clusterisation model. We solve the Lippmann-Schwinger equations assuming that coupling effects between channels involving the ${}^2\text{H}$ bound 3S_1 state and those of the virtual 1S_0 state are negligible. Two calculations have been performed; one using a potential that best recreates the ${}^6\text{Li}$ spectrum, and the other to best recreate the low-energy elastic cross section, for which there is a large amount of experimental data. The potential so prescribed in each case is used for both the 3S_1 and 1S_0 channel sets. These calculations show that an effective two-body model suffices to explain many features of the data.

The 26th International Nuclear Physics Conference

11-16 September, 2016

Adelaide, Australia

*Speaker.

1. Introduction

Many experiments have measured the cross section for low-energy elastic scattering of ²H and ⁴He, dating back to the 1930s [1]. The data show three states of the compound nucleus, ⁶Li, which appear as resonances: a 3⁺;0 at 0.7117 MeV above the scattering threshold in the centre-of-mass frame, a 2⁺;0 at 2.8357 MeV above threshold, and a less-pronounced 1⁺;0 at 4.1757 MeV above threshold. Early theoretical methods used to recreate this data involved parameter fitting with no nuclear model input. Recently, more sophisticated approaches have been used, included solving the Alt-Grassman-Sandhas (AGS) three-body equations [2], and an *ab-initio* microscopic model using two- and three-nucleon forces to take into account the motion of all six nucleons of the two bodies [3, 4, 5, 6].

However, it is instructive to see which features of the data may be explained at a two-body level. Such an approach was recently used to calculate phase shifts for this system, and the *S*-factor for capture [7], but not the compound spectrum or elastic scattering cross section.

As we are concerned with the first few MeV above threshold, and the first excited state of ⁴He has an energy of 20 MeV, we treat it as a spin-zero structureless boson. We construct channels with its ground state and the ²H ³S₁, *T* = 0 (ground) state and ¹S₀ *T* = 1 (excited) state. The latter is usually expected to be a resonance above the *p* – *n* break-up threshold, with an energy that is not firmly known. However, a bound state description of it at –67 keV has been contemplated [8], and we use this energy herein. We assume the coupling between the two states of different isospin to be negligible, and so the channels formed with the ¹S₀ state are not coupled to those formed with the ³S₁ state. As there is no mixing of channels involving different ²H states, all compound-system states found are orthogonal. Thus, spurious states, if found, may be simply discarded.

2. Formalism

We performed scattering calculations by solving momentum-space Lippmann-Schwinger equations

$$T_{cc'}^{J^\pi}(p, q; E) = V_{cc'}^{J^\pi}(p, q) + \mu \sum_{c''} \int_0^\infty V_{cc''}^{J^\pi}(p, x) \frac{x^2}{k_{c''}^2 - x^2 + i\epsilon} T_{c''c'}^{J^\pi}(x, q; E) dx, \quad (2.1)$$

where *E* is projectile energy, *p* and *q* are momentum variables, *k* = √*μE* is the wave number, and *μ* is reduced mass. Assuming that the potentials, *V*_{*cc'*}^{*J*^π}, are separable (and *J*^π henceforth understood),

$$V_{cc'} = - \sum_p |\chi_{cp}\rangle \frac{1}{\eta_p} \langle \chi_{c'p}|, \quad (2.2)$$

the *T*-matrices also take a separable form,

$$T_{cc'} = - \sum_p |\chi_{cp}\rangle \frac{1}{[1 - \eta_p] \eta_p} \langle \chi_{c'p}|, \quad (2.3)$$

where the optimal expansion is in terms of Sturmian form factors, *χ*, and their eigenvalues *η* [9].

The potentials used have the form

$$V_{cc'} = V_{cc'}^{\text{coul}}(r) + f(r) [V_0 \delta_{cc'} + V_{\ell\ell} [\ell \cdot \ell]_{cc'} + V_{II} [I \cdot I]_{cc'}] + \frac{V_{\ell I}}{r} \frac{df(r)}{dr} [\ell \cdot I]_{cc'}, \quad (2.4)$$

with central potential V_0 , orbital angular momentum potential $V_{\ell\ell}$, spin-orbit potential $V_{\ell I}$, and spin-spin potential V_{II} , for channels c . The potential shapes are Woods-Saxon functions,

$$f(r) = [1 + e^{(\frac{r-R}{a})}]^{-1}, \quad (2.5)$$

where a and R are constants of diffuseness and radius at half-maximum. As only positive parity states have been observed in ⁶Li, the interaction potentials used contain only positive parity components. The Coulomb potentials, $V_{cc'}^{\text{coul}}(r)$, are determined by using a three-parameter Fermi (3pF) distribution for each cluster, and these are folded together [10]. The 3pF distributions are defined by the experimentally known root-mean-squared charge radii [11].

We also allowed the potential to have quadrupole deformation. To do this, the Woods-Saxon potentials are deformed such that the radius has an angular dependence, i.e. $R(\theta, \phi) = R_0[1 + \varepsilon]$, where

$$\varepsilon = \sum_{L \geq 2} \beta_L \sqrt{\frac{4\pi}{2L+1}} [\mathbf{Y}_L(\Omega) \cdot \mathbf{Y}_L(\hat{Y})]. \quad (2.6)$$

Y are the Euler angles for the transformation from the body-fixed frame and Ω are the angles defining the surface in the space-fixed frame. Full details of the expansion are in Ref. [12].

3. Results and Discussion

We have found two parameter sets, one optimised to recreate the ⁶Li spectrum and another optimised to recreate cross sections of the ²H(α, α)²H reaction. These are denoted as calculation 1 and calculation 2, respectively. Fig. 1 shows the experimental spectrum of ⁶Li compared with the results of these calculations.

In calculation 1 (2), the central potential, V_0 , had a depth of -59.63 (-64.775) MeV. The orbital angular momentum term, $V_{\ell\ell}$, had a depth of 0.12303 (0.93) MeV. The term dependent on the ²H states' angular momentum, V_{II} , had a depth of -26.525 (-2.0) MeV. Finally, the spin-orbit term, $V_{\ell I}$, had a depth of 2.08 (1.97). In both of these calculations, $\beta_2 = 0.22$ for both ²H states.

In calculation 1, all state centroids are within ~ 100 keV of their measured counterparts except for the $2^+;0$ state, which has a calculated energy that is 800 keV too large. In calculation 2, the $0^+;1$ and $1_2^+;0$ states are each ~ 1 MeV too low in energy, whereas the $2^+;0$ has the correct energy. The fact that such a large V_{II} term was required in calculation 1 to correctly place the $0^+;1$ and $1_2^+;0$ states, and that such a value worsens agreement of the $2^+;0$ state, suggests that some elaboration on the potential is required. To improve the $T = 1$ states, it is reasonable to assume that the potential of the ²H singlet state should differ from that of the triplet, but here we have used the same potential for both to reduce the number of free parameters. That the 1^+ state is recreated well by the six-body calculation of Ref. [5] but not here suggests a limitation of the two-body approach.

Seeing that the $3^+;0$ and $2^+;0$ states are the most pronounced resonances in the experimental cross sections for ²H-⁴He scattering, these two states and the ground state were focused upon when adjusting the potential parameters of calculation 2, to achieve cross sections better matching data. Figs. 2 and 3 show the resulting cross sections from calculations 1 and 2 for one selected fixed angle and several fixed energies, respectively.

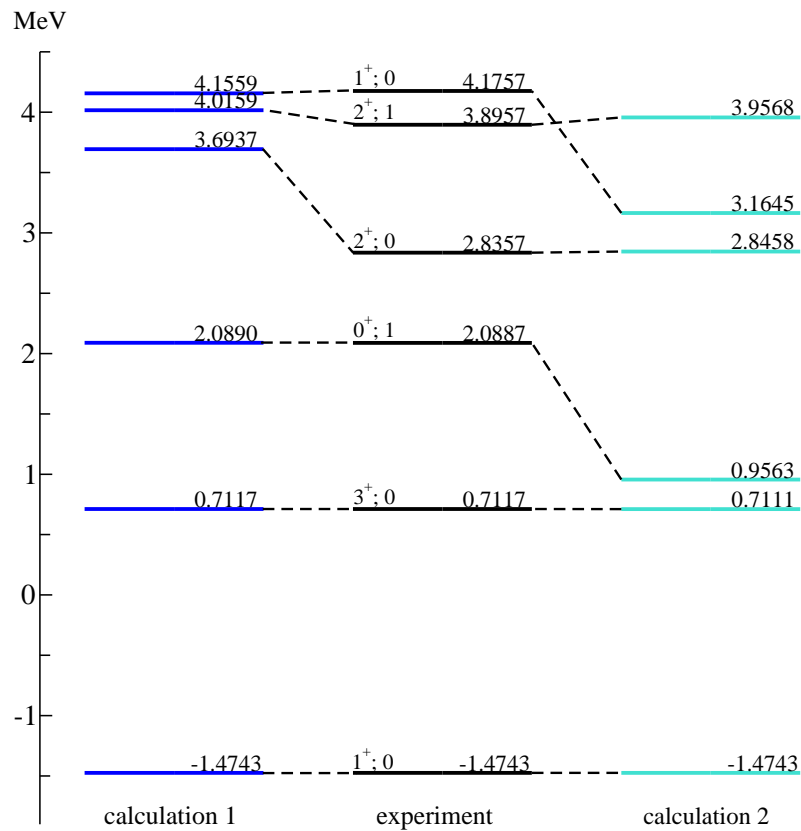


Figure 1: Experimental and calculated spectra of ${}^6\text{Li}$. Data from Ref. [13].

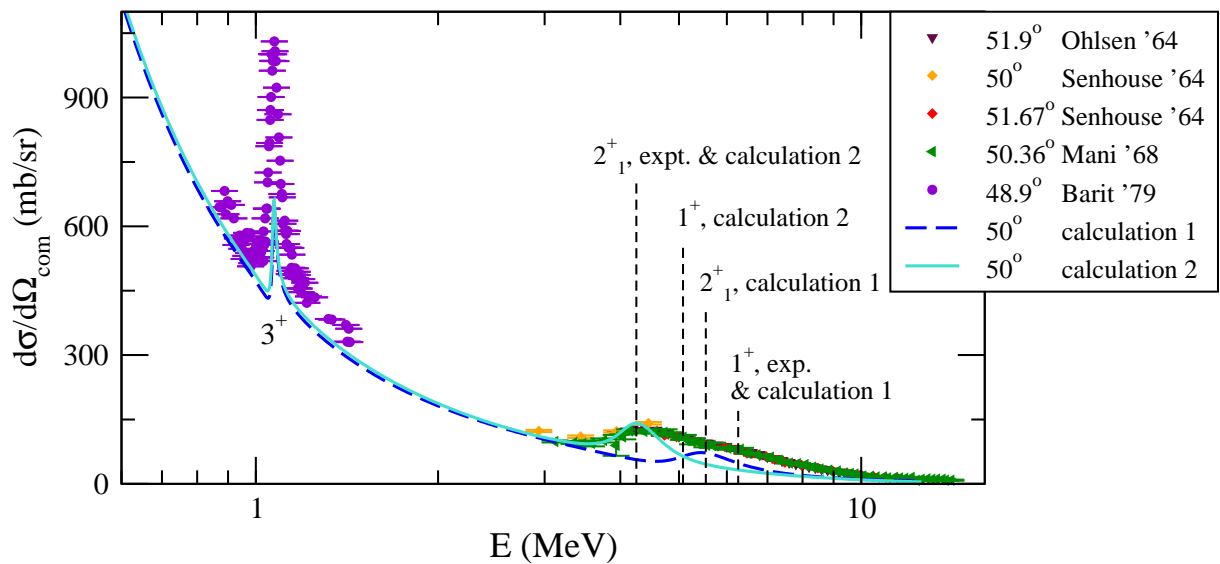
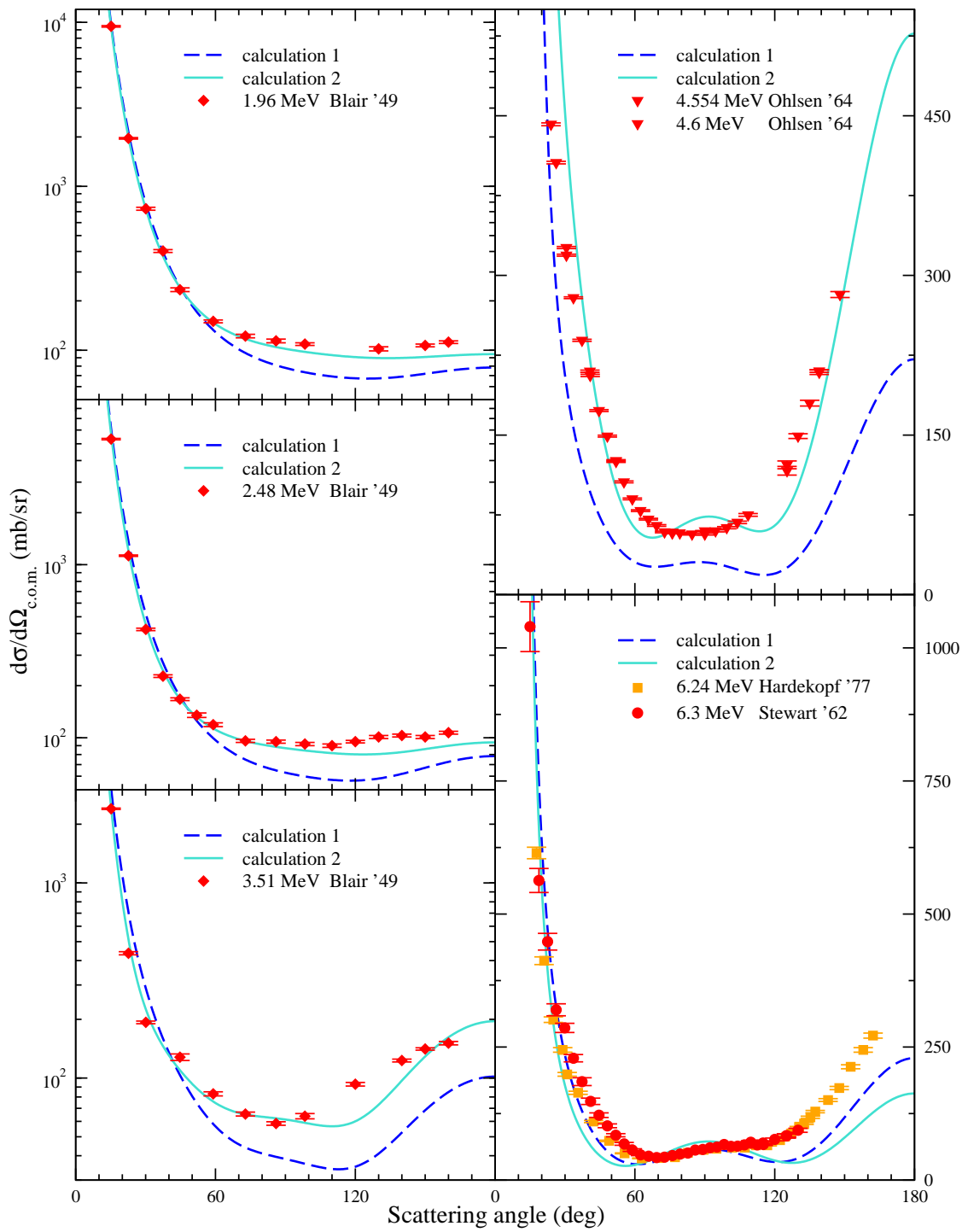


Figure 2: Fixed-angle cross sections at 50° determined by calculation 1 (dashed line) and calculation 2 (solid line) compared with the experimental cross sections from Refs. [14, 15, 16, 17].



POS (INPC2016) 204

Figure 3: Fixed energy cross sections at 1.96, 2.48, 3.51, 4.6 and 6.3 MeV by calculation 1 (dashed line) and calculation 2 (solid line) compared with the experimental cross sections from Refs. [14, 18, 19, 20].

Both spectra and cross sections determined by calculations 1 and 2 show good agreement with the experimental data. The 3^+ resonance is well reproduced in both calculations. The cross sections determined by calculation 2 better match the experimental data, as the energy of the $2^+;0$ state is better reproduced. The underestimation of the cross section around 6 MeV in both calculations is due to the absence of the $1^+;0$ resonance, which is found in the calculated spectrum but not in the calculated cross section. This resonance is well reproduced in Ref. [5], suggesting another limitation of the two-body approach.

4. Conclusions and Future Considerations

We have investigated elastic scattering of ^4He with ^2H using a two-body clusterisation model. Two different potentials were used, one to best recreate the lowest six states of the ^6Li spectrum, and the other is optimised to reproduce experimental cross section data. The results of both calculations show good agreement with the experimental data, and indicate that an effective two-body model can explain most, but not all, observed features of the system. These calculations will be used in future studies to determine capture cross sections in $^2\text{H}-^4\text{He}$ collisions, using the method outlined in Ref. [21].

Acknowledgments

This work is supported by U.S. National Science Foundation under Award No. PHY-1415656. DWD acknowledges the support of the ARC Centre of Excellence for Nanoscale BioPhotonics (CE140100003).

References

- [1] E. Pollard and H. Margenau, *Phys. Rev.* 47, 833 (1935). (1968).
- [2] A. Deltuva, *Phys. Rev. C* 74, 064001 (2006).
- [3] S. Quaglioni and P. Navrátil, *Phys. Rev. Lett.* 101, 092501 (2008).
- [4] P. Navrátil and S. Quaglioni, *Phys. Rev. C* 83, 044609 (2011).
- [5] G. Hupin, S. Quaglioni, and P. Navrátil, *Phys. Rev. Lett.* 114, 212502 (2015).
- [6] P. Navrátil et al., *Physica Scripta* 91, 053002 (2016).
- [7] S. B. Dubovichenko and Yu. N. Uzikov, *Phys. Part. Nucl.* 251, 42 (2011).
- [8] S. B. Borzakov, N. A. Gundorin, and Y. N. Pokotilovski, *Phys. Part. Nuclei Lett.* 12, 536 (2015).
- [9] K. Amos et al., *Nucl. Phys. A* 728, 65 (2003).
- [10] K. Amos et al., arXiv:1612.04192 (2017).
- [11] C. W. De Jager and H. De Vries and C. De Vries, *Atomic Data and Nuclear Data Tables*, 14 (1974).
- [12] P. R. Fraser et al., *Phys. Rev. C* 90, 024616 (2014).
- [13] D. R. Tilley et al. *Nucl. Phys. A* 708, 3 (2002).
- [14] G. G. Ohlsen and P. G. Young, *Nucl. Phys.* 52, 134 (1964).

- [15] L. Senhouse and T. Tombrello, Nucl. Phys. 57, 624 (1964).
- [16] G. Mani and A. Tarratts, Nucl. Phys. A107, 624 (1968).
- [17] I. Y. Barit et al., Soviet J. Nucl. Phys. 29, 585 (1979).
- [18] J. M. Blair, G. Freier, E. E. Lampi, and W. Sleator, Phys. Rev. 75, 1678 (1949).
- [19] L. Stewart, J. E. Brolley, and L. Rosen, Phys. Rev. 128 (1962).
- [20] R. A. Hardekopf et al., Nucl. Phys. A287, 237 (1977).
- [21] L. Canton and L. G. Levchuk, Nucl. Phys. A808, 192 (2008).